Developmental and Comparative Immunology 35 (2011) 937–948

Contents lists available at ScienceDirect

Developmental and Comparative Immunology

journal homepage: www.elsevier.com/locate/dci

Antisense approaches for elucidating ranavirus gene function in an infected fish cell line

D.S. Whitley[a], R.C. Sample[a,1], A.R. Sinning[b], J. Henegar[c], V.G. Chinchar[a,*]

[a] Department of Microbiology, University of Mississippi Medical Center, 2500 North State Street, Jackson, MS 39216, United States
[b] Department of Anatomy, University of Mississippi Medical Center, 2500 North State Street, Jackson, MS 39216, United States
[c] Department of Pathology, University of Mississippi Medical Center, 2500 North State Street, Jackson, MS 39216, United States

ARTICLE INFO

Article history:
Available online 13 December 2010

Keywords:
Antisense morpholino oligonucleotides
asMO
siRNA
RNA interference
Ranavirus
Frog virus 3
Viral gene function

ABSTRACT

Viral virulence/immune evasion strategies and host anti-viral responses represent different sides of the continuing struggle between virus and host survival. To identify virus-encoding molecules whose function is to subvert or blunt host immune responses, we have adapted anti-sense approaches to knock down the expression of specific viral gene products. Our intention is to correlate knock down with loss of function and thus infer the role of a given viral gene. As a starting point in this process we have targeted several structural and catalytic genes using antisense morpholino oligonucleotides (asMO) and small, interfering RNAs (siRNA). In proof of concept experiments we show the feasibility of this approach and describe recent work targeting five frog virus 3 genes. Our results indicate that both 46K and 32R, two immediate-early viral proteins, are essential for replication *in vitro*, and confirm earlier findings that the major capsid protein, the largest subunit of the viral homolog of RNA polymerase II, and the viral DNA methyltransferase are also essential for replication in cell culture.

1. Introduction

> "Through millennia of co-evolution, pathogens have acquired substantially more insight into the complexity of host immune responses than human immunologists."
> Rowland-Jones S and Dong T. Science 443:282–283 (2006)

Although viruses are intrinsically interesting to virologists, they also attract the attention of immunologists (or at least that subgroup known as "viral immunologists") because of their ability to evade specific elements of the host's immune defense system and, in that way, illuminate the role of those elements in anti-viral immunity. Understanding the precise roles that innate and acquired responses play in anti-viral immunity is challenging, but the observation that viruses encode proteins that inhibit specific immune pathways provides "biological proof" for the importance of those responses in host defense. Moreover, because host anti-viral defense mechanisms and virus-encoded virulence genes likely represent different sides of the same coin, elucidating key elements of the anti-viral response requires not only a thorough understanding of the genetics of the host's immune system, but also a detailed understanding of viral gene function. Herein we describe an anti-sense approach designed to elucidate viral gene function.

Although the broad outlines of frog virus 3 (FV3, genus *Ranavirus,* family Iridoviridae) replication are known, the precise details of viral macromolecular synthesis, virion assembly, and virulence are only imperfectly understood (reviewed in Chinchar et al., 2009). Understanding ranavirus replication and pathogenesis is important because members of this genus adversely impact a wide-variety of cold-blooded animals. For example, ranaviruses such as Frog virus 3, *Ambystoma tigrinum* virus, and Epizootic haematopoetic necrosis virus have been linked to localized die-offs among frogs, salamanders, and fish (Cunningham et al., 1996; Duffus et al., 2008; Gray et al., 2009; Green et al., 2002; Greer et al., 2005; Jancovich et al., 1997; Jensen et al., 2009), and members of another genus (*Megalocytivirus*) within the family Iridoviridae are responsible for wide-spread die-offs among cultured fish in Asia (Weber et al., 2009). Moreover, despite the observation that many iridovirid (a term denoting members within all five gen-

Abbreviations: asMO, antisense morpholino oligonucleotide; C_T, threshold crossing value; DMEM, Dulbecco's modified Eagle's medium; DMT, DNA methyltransferase; dsRNA, double-stranded RNA; FHM, fathead minnow; FV3, frog virus 3; FNS-CTL, fluorescein-tagged non-silencing control; FV3-RFP, an FV3 recombinant that expresses red fluorescent protein; HMEM, Eagle's minimum essential medium with Hank's salts; MCP, major capsid protein; MOI, multiplicity of infection; mol wt, molecular weight; NFH, neurofilament triplet heavy chain protein; NTC, non-targeting negative control; PFU, plaque forming units; p.i., post infection; RNAi, RNA interference; qRT-PCR, quantitative real-time polymerase chain reaction; SDS-PAGE, sodium dodecyl sulfate polyacrylamide gel electrophoresis; siRNA, small interferring RNA; vPol-IIα, viral homolog of the largest subunit of RNA polymerase II.

* Corresponding author. Tel.: +1 601 984 1743; fax: +1 601 984 1708.
E-mail address: vchinchar@umc.edu (V.G. Chinchar).
[1] Current address: Department of Biology, Mississippi College, Clinton, MS, United States.

0145-305X/$ – see front matter © 2010 Elsevier Ltd. All rights reserved.
doi:10.1016/j.dci.2010.12.002

era of the family Iridoviridae) genes are conserved among diverse members of the family, the specific functions of most viral gene products are unknown (Eaton et al., 2007). Iridovirid genes fall into three categories: essential, efficiency/host range, and virulence/immune evasion. As the name implies, essential genes are absolutely required for virus replication in all cells. Essential genes include the virus-encoded DNA polymerase, homologs of the two largest subunits of RNA polymerase II, and structural and non-structural proteins that play critical roles in virion assembly. Efficiency/host range genes are those which enhance replication in all cell types, or are required for replication in specific cell types, but whose deletion does not invariably abolish replication *in vitro*. Efficiency/host range genes are thought to include genes that play a role in nucleotide biosynthesis, e.g., thymidylate synthase, dUTPase, dihydrofolate reductase, and ribonucleotide reductase. Lastly, virulence/immune evasion genes are those which allow the virus to replicate *in vivo* (and in some cases *in vitro*) by blocking host anti-viral responses. Based on homology to other phylogenetically related nucleo-cytoplasmic large DNA viruses such as poxviruses, ascoviruses, phycodnaviruses, and African swine fever virus (Alcami and Koszinowski, 2000; Johnston and McFadden, 2003), we postulate that iridovirids contain a half dozen or more genes whose function is to circumvent various aspects of the host immune response (see below). In view of these gaps in our knowledge of viral gene function, our goal is to elucidate the role that viral genes play using anti-sense approaches. Moreover, this study bridges the disciplines of virology and immunology since elucidating the identity and function of virus-encoded immune evasion molecules will likely identify specific elements of the host immune response that play critical roles in anti-viral immunity.

Within the family Iridoviridae, a half dozen or more putative virulence/immune evasion genes have been tentatively identified by homology to similar proteins in other viruses (Tidona and Darai, 1997; He et al., 2002; Jancovich et al., 2003; Tan et al., 2004; Song et al., 2004; Tsai et al., 2005; Huang et al., 2009). In FV3 and related ranaviruses, candidate immune evasion/virulence genes include a viral homolog of the largest subunit of eukaryotic initiation factor 2, a β-hydroxysteroid dehydrogenase homolog, a ribonuclease III (RNase)-like protein, a cytosine DNA methyltransferase (DMT), and a virus-encoded caspase activation and recruitment domain containing protein. Ranaviruses and other members of the family contain additional putative immune evasion genes, e.g., a tumor necrosis factor receptor homolog, several putative proteins with immunoglobulin-like domains, homologs of semaphorin, and putative antagonists of apoptosis (Eaton et al., 2007). Moreover, since the above genes were identified by amino acid sequence identity/similarity with their well-characterized mammalian counterparts, it is likely that other, less conserved, immune evasion proteins remain to be discovered. Identifying the precise function of these genes is important for understanding viral replication *in vivo*. In addition, determining the precise function of these genes within infected cells, and more importantly within infected animals, will provide key insights into the anti-viral immune response of lower vertebrates. Although recent work has markedly expanded our knowledge of immunity among model fish and amphibians and shown that amphibian and fish immune systems are functionally similar to those of higher vertebrates, salient differences have been noted (Litman et al., 2010). For example, cytokine genes such as interferon often show only minimal sequence relatedness to their mammalian counterparts, likely reflecting 300–400 million years of divergent evolution and responsiveness to different pathogens (Long et al., 2004). In addition, unique surface receptor molecules, e.g., leukocyte immune-type receptors and novel immune type receptors in fish and novel FcR-like molecules in *Xenopus*, are present in lower vertebrates, but not in birds or mammals (Stafford et al., 2007; Guselnikov et al., 2008; Litman et al., 2010).

We are interested in developing methodologies for identifying viral genes that antagonize anti-viral host responses among lower vertebrates. For this study, we have chosen FV3 because it is one of the best characterized pathogens of lower vertebrates and because suitable *in vitro* and *in vivo* systems are available to examine replicative and immune-related events (Gantress et al., 2003; Chinchar et al., 2009; Morales et al., 2010). To accomplish this task, we have chosen in our initial experiments to identify the role of putative structural and catalytic genes by knocking down their expression and discerning function by changes in phenotype using an antisense approach. To date we and others have successfully knocked down the expression of four viral genes using anti-sense morpholino oligonucleotides (asMOs) and siRNA (Xie et al., 2005; Sample et al., 2007; Whitley et al., 2010). Mechanistically, asMOs inhibit translation by binding to target mRNAs at, or upstream of, the initiating AUG codon and blocking ribosomal scanning (reviewed in Ekker and Larson, 2001), whereas siRNAs block gene expression either by binding and degrading target messages or by interfering with translation (Meister and Tuschl, 2004; Appasani, 2011)). In the case of siRNAs, binding is mediated by the RNA induced silencing complex and leads to activation of a complex-associated ribonuclease that cleaves the targeted RNA. Moreover, whereas the asMO target is limited to the 5′ non-translated region or the immediate vicinity of the start codon, siRNA target sites may lie within any coding or non-coding region within the message. The results of our initial experiments support the utility of these approaches *in vitro*. Recent work is described below as are directions for further research and the strengths and weaknesses of this approach.

2. Materials and methods

2.1. Cells and virus

FV3 infections were performed in fathead minnow cells (FHM, American Type Culture Collection, ATCC No. CCL-42) grown in Dulbecco's modified Eagle's medium (DMEM) containing 4% fetal bovine serum at 26 °C in a humidified incubator in 95% air and 5% CO_2. FV3 (Granoff et al., 1965; ATCC VR-569) and a FV3 recombinant that constitutively expresses red fluorescent protein and replicates comparably to *wt* FV3 (FV3-RFP, Jacques Robert, University of Rochester School of Medicine) were propagated on confluent monolayers of FHM cells grown in 150 cm^2 flasks and incubated in Eagle's minimum essential medium with Hank's salts (HMEM) supplemented with 4% fetal bovine serum. To generate virus stocks, FHM cells were infected at a multiplicity of infection (MOI) of ~0.01 plaque forming units (PFU)/cell and harvested ~5 days later when cytopathic effect was marked. Virions were released by three freeze–thaw cycles and the virus-containing supernatant clarified by low speed centrifugation. Virus titers were determined by plaque assay on FHM monolayers under an overlay of 0.75% methylcellulose.

2.2. Antisense morpholino oligonucleotides

AsMOs and delivery agents were purchased from GeneTools (Philomath, OR) and were used according to the manufacturer's protocol. Four different morpholino oligonucleotides were utilized: a non-targeting negative control (NTC) (5′CCTCTTACCTCAGTTACAATTTATA3′), an asMO targeting the major capsid protein (MCP) (5′TGAACCAGTTACAGAAGA**CAT**TTCC3′) as a positive control, an asMO targeting the 46K protein (46K) (5′ GAGAGTCTGTCACAAAGTTTGC**CAT** 3′), and an asMO targeting the

32R protein (32R) (5′ CCCTCAGTTCAGTAACAGTAAC**CAT** 3′). As indicated by underlining and boldface type, the anti-MCP, anti-46K, and anti-32 asMOs bound slightly upstream of, or precisely at, the AUG initiation codon. AsMOs were used at a final concentration of 10 μM and the delivery agent Endo-Porter was used at a final concentration of 6 μM.

2.3. FV3 protein synthesis

FHM cells were grown to ~80% confluency (~1.9×10^6 cells/well) in 6 well tissue culture plates. On the day of assay, the media was removed by aspiration and replaced with 1 mL of DMEM containing 4% fetal bovine serum. Subsequently, 6 μL of Endo-Porter and 10 μL of a 1 mM stock of the indicated asMO were added, and the cultures incubated at 26 °C. Twenty-four hours after treatment, the cultures were infected with FV3 at a MOI of 20 PFU/cell. To detect viral proteins, replicate cultures were radiolabeled with methionine–cysteine free Eagle's minimum essential medium with Earle's salts containing 30 μCi/mL [^{35}S] methionine-cysteine (EasyTag Express Protein Labeling Mix, Perkin-Elmer) from 7 to 9 h post infection (p.i.). At 9 h p.i., the radiolabeled medium was removed, and cell lysates were prepared by disrupting the cells in 300 μL direct sample buffer (125 mM Tris–HCl, pH 6.8, 10% glycerol, 2% SDS, 0.02% 2-mercaptoethanol, 0.01% bromophenol blue). Radiolabeled proteins were separated by electrophoresis on 10% SDS-polyacrylamide gels (Laemmli, 1970), and visualized by autoradiography using Kodak XAR film or by phosphoroimaging (BioRad, Personal Molecular Imager).

2.4. FV3 viral yields

To determine virus yields viral growth was stopped by freezing the cultures at the indicated times (24 h p.i. for asMO experiments and 48 h p.i. for siRNA studies). Virions were released by three cycles of freeze–thaw and cellular debris removed by low speed centrifugation. Clarified, virus-containing supernatants were serially diluted 10-fold and 200 μL of each dilution was added to duplicate wells of confluent FHM monolayers grown on 6 well plates. After a 1 h absorption period, the cells were overlaid with 2 mL of DMEM containing 2% fetal bovine serum and 0.75% methyl cellulose. After 7 days, the overlay was removed and plaques were visualized by staining with 1% crystal violet in 70% ethanol.

2.5. RNA interference (RNAi)

siRNAs targeting three FV3 transcripts (those encoding the MCP, DMT, and the largest subunit of the viral homolog of RNA polymerase II, vPol-IIα) were designed using an algorithm supplied by the manufacturer and purchased from Dharmacon RNAi Technologies (Lafayette, CO). In addition, a siRNA similar to one targeting the tiger frog virus MCP was also designed (Table 1; Xie et al., 2005). Two non-silencing siRNAs were used as negative controls and to monitor transfection efficiency: a DY-547 tagged siGLO Red® RISC-free control (siGLO; Dharmacon RNAi Technologies) and a fluorescein tagged non-silencing control (FNS-CTL; Qiagen, Germantown, MD). Synthetic siRNAs were provided as desalted, lyophilized pellets and were rehydrated in siRNA buffer (300 mM KCL, 30 mM HEPES, pH 7.5, and 1.0 mM $MgCl_2$) to yield a working stock of 20 μM.

FHM cells were plated at ~50% confluency (1×10^6 cells/well; 6 well dishes) in DMEM containing 5% fetal bovine serum and incubated in a humidified incubator in 95% air/5% CO_2 at 25 °C. FHM cells were transfected 24 h after plating with media containing 50 nM siRNAs using DharmaFECT 1 (Dharmacon) as the transfection reagent. Briefly, 150 μL of serum free media was combined with 50 μL of 2 μM siRNA in a 12 mm × 75 mm polystyrene tube. At the same time, 196 μL serum free media was combined with 4 μL DharmaFECT1 in a second 12 mm × 75 mm polystyrene tube. Both tubes were incubated at room temperature for 5 min, their contents combined and incubated at room temperature for an additional 20 min before adding 1.6 mL of DMEM with 5% fetal bovine serum. Two mL of growth medium containing siRNA/DharmaFECT1 complexes were added to FHM monolayers and the cultures were incubated as described above. Approximately 24 h later the cells were infected with FV3-RFP at MOIs ranging from 0.01 to 10.0 PFU/cell. After allowing 1 h for adsorption, non-attached virus was removed by washing and the cultures were incubated as described above. The infection was stopped at 48 h p.i., and replicate cultures processed for RNA extraction, transmission electron microscopy, and plaque assay.

Table 1
siRNA sequences.

siRNA	Orientation	Sequence
FNS-CTL[a]	Sense	UUCUCCGAACGUGUCACGUdTdT
	Antisense	dTdTAAGAGGCUUGCACAGUGCA
siGLO-CTL[b]	Sense	N/A
	Antisense	N/A
Anti-MCP-4[c]	Sense	**A**CGCCUGGUUGGU**G**CUCAAdTdT
	Antisense	dTdT**T**GCGGACCAACCA**C**GAGUU
Anti-vPol-1	Sense	GGAAAUGUUUGCAUCUAAAdTdT
	Antisense	dTdTCCUUUACAAACGUAGAUUU
Anti-DMT-1	Sense	UGGCCGACUCUGACUAUAA dTdT
	Antisense	dTdTACCGGCUGAGACUGAUAUU

[a] FNS-CTL is an FITC-labeled non-silencing control siRNA (Qiagen).
[b] siGLO-CTL is a non-RISC incorporated control that is labeled with the dye DY-547 (Dharmacon, Fafayette, CO).
[c] This sequence is similar but not identical to the Si1 siRNA designed by Xie et al. (2005). Anti-MCP-4 contains the addition of a 5′ terminal A residue, the deletion of the 3′ terminal C residue, and the substitution of a G (found in FV3) for an A (found in tiger frog virus) at position 14 of the sense strand. The above changes on the sense and anti-sense strands are indicated by boldface type.

2.6. RNA extraction and qRT-PCR analysis

Total cellular RNA was isolated from FHM cells using Trizol (Invitrogen, Carlsbad, CA) and cDNA was synthesized from 1 μg of total RNA using the iScript cDNA synthesis kit (Bio-Rad, Hercules, CA). Expression levels of viral genes in relation to a standard (FHM 18S rRNA) were determined based on C_T (threshold crossing) values using the $2^{-\Delta\Delta C_T}$ method of Livak and Schmittgen (2001). Because this calculation involved comparison of transcript levels in mock and virus infected cells, a C_T value of 30 was chosen as the background level for viral gene expression in mock-infected samples. qRT-PCR primers (Table 2) targeting viral genes encoding MCP, vPol-IIα, and DMT and FHM 18S rRNA (control) were designed using DNASTAR (Madison, WI).

To confirm the suitability of primer pairs for qRT-PCR, cDNA of three different dilutions (undiluted, 1/10, and 1/100 diluted in

Table 2
qRT-PCR primers.

Primer designation	Primer sequence (5′–3′)
FHM 18S rRNA F-Q[a]	CCGCAGCTAGGAATAATGGA
FHM 18S rRNA R-Q	CATCGTTTACGGTCGGAACT
FV 3 Major Capsid Protein F-Q	CCTCCCCTACAACGAGATCA
FV 3 Major Capsid Protein R-Q	CAACCATGTCCCTGACTGTG
FV 3 cytosine DNA-methyltransferase F-Q	ACACGGGTCGCATGAAAGAG
FV 3 cytosine DNA-methyltransferase R-Q	GGTCCAACAGCTCCACAATAA
FV 3 viral RNA Polymerase-IIα F-Q	ACGGACAGGATGATGAGGAG
FV3 viral RNA Polymerase-IIα R-Q	CTCCTCATCATCCTGTCCGT

[a] Primer designations: the target transcript is indicated; Q denotes a quantitative real-time PCR primer; F, forward primer; R, reverse primer.

nuclease free water) from the CTL sample was combined with each of the primer pairs, including that for FHM 18S rRNA. To verify the quality of cDNAs used, FHM 18S rRNA primers were used to amplify CTL and treated cDNA samples at the dilutions indicated above. Relative gene expression was determined only when the efficiency of reactions amplifying the gene of interest and the housekeeping gene were found to be approximately equivalent. All reactions were performed in triplicate in a total volume of 25 μL. Each 25 μL reaction consisted of 12.5 μL of 2× SYBR green Supermix (100 mM KCl, 40 mM Tris–HCl pH 8.4, 0.4 mM of each dNTP, 0.5 unit *Taq* DNA polymerase, 6 mM $MgCl_2$, 20 nM fluorescein, Bio-Rad, Hercules, CA), 0.5 μL each of forward and reverse primers (0.5 μM each), 1 μL cDNA (diluted as indicated above) and 10.5 μL sterile nuclease-free water. The cycling conditions were 1 cycle at 95 °C for 1 min followed by 30 cycles of 95 °C for 20 s and 55 °C for 1 min. Data were collected during the 1 min annealing/extension step. To verify that a single product was synthesized, melt curves were generated for each product and only primer pairs and cDNAs that generated a single peak were used in the final analyses. Cycling conditions for melt curve analysis were 1 cycle at 95 °C for 1 min followed by 1 cycle at 50 °C for 1 min and 100 cycles at an initial temperature of 50 °C and increasing stepwise by 0.5 °C thereafter to a final temperature of 100 °C with a cycle duration of 10 s.

2.7. Transmission electron microscopy

FV3-infected cultures were processed for transmission electron microscopy as described earlier (Sample et al., 2007). At the indicate times post infection, the medium was removed and the cells rinsed gently with 0.1 M sodium phosphate, pH 7.4. The cells were scraped into fresh buffer, pelleted, fixed in 2% glutaraldehyde in 0.1 M sodium phosphate buffer, and stored at 4 °C until processed for electron microscopy. At that time, the samples were post fixed in 1% osmium tetroxide and stained with 2% uranyl acetate in de-ionized water. The samples were dehydrated in a stepwise fashion in ethanol, the ethanol removed by treatment with 100% propylene oxide, and the samples embedded in resin composed of 45% Epon, 19% NMA (methyl-5-norbornene-2,3-dicarboxylic anhydride), and 36% DDSA (dodecenyl succinic anhydride). Thin sections (0.1 μm) were floated onto 200 mesh copper hexagonal grids (Electron Microscopy Science, Fort Washington, PA), counter-stained with lead citrate, and examined using a Leo 906 (Zeiss) transmission electron microscope.

3. Results

3.1. asMO-mediated knock down of viral gene function

Gene-specific asMOs have been used to knock down the expression and infer functions of the FV3 major capsid protein, the viral homolog of the largest subunit of RNA polymerase II (vPol-IIα), and ORF 53R, a virus-encoded putative myristoylated membrane protein (Sample et al., 2007; Whitley et al., 2010). Here we use this technique to determine the *in vitro* requirement for two FV3 immediate early genes of unknown function, 46K (ORF 91R) and ORF 32R (Tan et al., 2004; Majji et al., 2009). The former has a predicted mol wt of ~46 kDa (p*I* = 5.5), and PSI-BLAST analysis indicates 46 K shares amino acid sequence identities and similarities with members of the T4 RNA ligase superfamily (Altschul et al., 1997). Blast analysis of the latter shows that 32R (mol wt 70 kDa, p*I* 9.96) shares homology with neurofilament triplet H1 (NFH)-like proteins, which are high mol wt proteins that are structural components of mammalian neurons (Lee and Cleveland, 1996; Tan et al., 2004; Perrot et al., 2008).

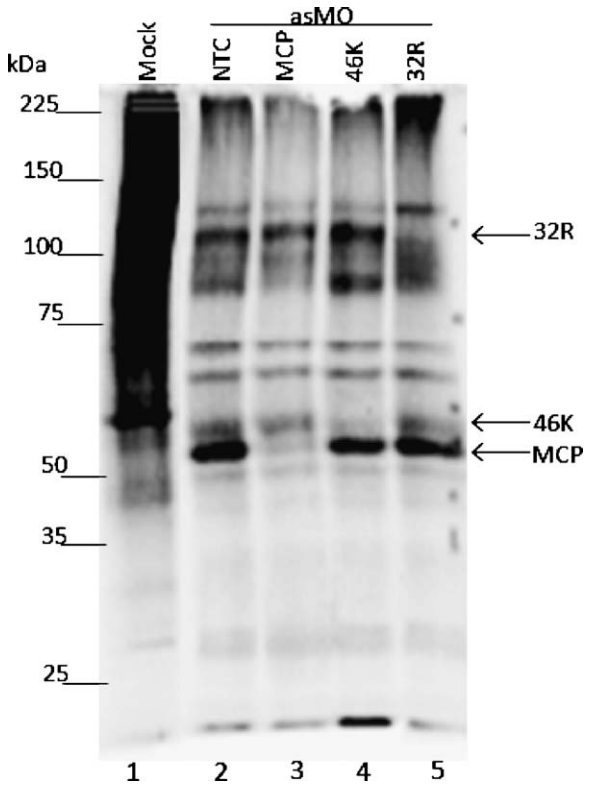

Fig. 1. SDS-PAGE analysis of asMO-treated, FV3-infected FHM cells. Mock-infected (lane 1) and virus-infected FHM cells were pre-treated with the indicated asMOs (lanes 2–5) and protein synthesis monitored 7–9 h p.i. Radiolabeled proteins were separated by 10% SDS-PAGE and visualized by phosphoroimaging. Positions of the MCP, 46K, and 32R proteins are indicated by arrows. Molecular weight markers (kDa) are shown to the left of the gel image. Lane headings here and elsewhere refer to FV3-infected cells pretreated with a non-targeting control (NTC), and asMOs targeted to the major capsid protein (MCP), 46K protein (46K), and 32R protein (32R).

In order to ascertain a function for these proteins, we blocked their expression using gene-specific asMOs and observed the effect of knock down on protein expression, FV3 replication, and virion assembly. Twenty-four hours prior to infection, FHM cells were pretreated with asMOs targeting either the 46K or 32R messages. In addition, a non-targeting control (NTC) asMO and a MCP-targeting asMO were used as negative and positive controls, respectively. Pretreated cells were infected with FV3 at a MOI of 20 PFU/cell and viral protein synthesis, monitored by pulse labeling with [^{35}S]methionine from 7 to 9 h p.i., was analyzed by SDS-PAGE. Treatment with the non-targeting control prior to infection had little to no effect on viral protein synthesis (Fig. 1, lane 2). Additionally, virus infection resulted in a marked inhibition of host cell protein synthesis and the appearance of characteristic FV3-specific proteins (compare lane 1, mock-infected cells, to lane 2, control treated, FV3-infected cells). As seen previously, treatment with an asMO targeting the MCP resulted in a marked reduction in the synthesis of the MCP without adversely affecting the synthesis of other viral proteins (lane 3). Treatment with asMOs targeting 46K resulted in a marked reduction of a ~50 kDa protein (lane 4), whereas 32R asMO treatment resulted in the reduction of a band >100 kDa in size (lane 5). Knockdown of neither the 46K nor 32R proteins had any observable effect on the synthesis of other viral proteins indicating that knockdown was limited to the target message. The failure to detect knock down of a 70 kDa protein, the predicted mol wt of the 32R product, and the loss of a much higher mol wt product was unexpected. As discussed below we speculate that phosphorylation of numerous serine residues within the 32R product resulted in its anomalous migration. This suggestion is

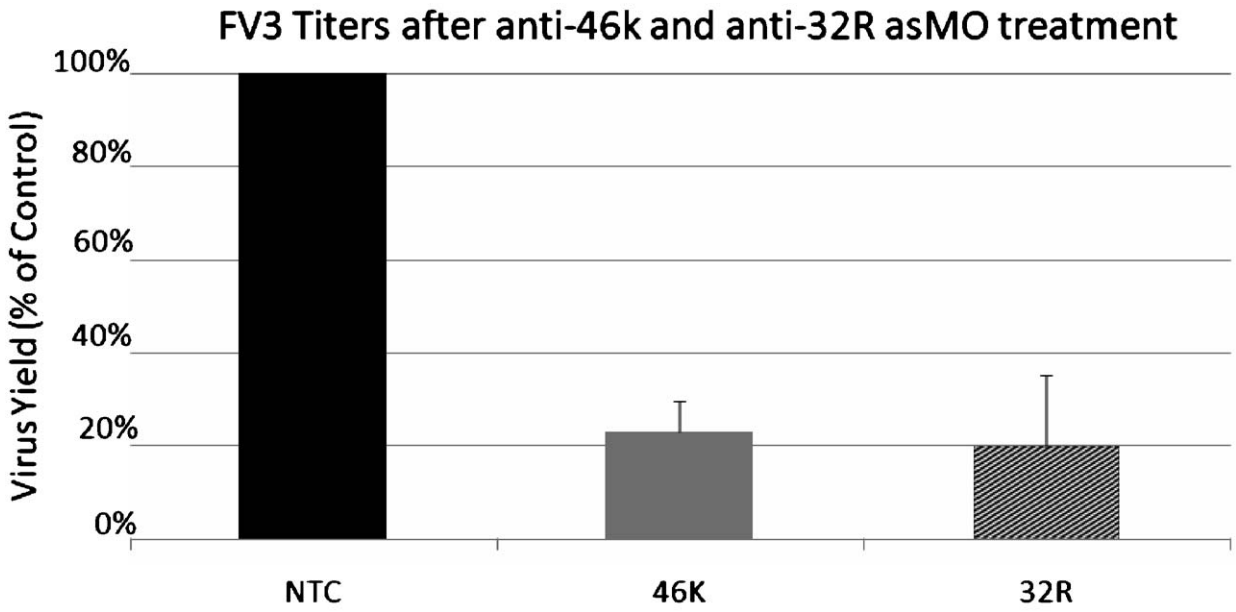

Fig. 2. FV3 yields following treatment with anti-46K and anti-32R asMO. FHM cells were treated with anti-46K or anti-32R asMOs 24 h prior to FV3 infection. At 24 h p.i., replication was stopped by freezing and viral yields determined by plaque assay. Shown are the averages and standard deviations of four replicate experiments from anti-46K and anti-32R treated cultures. Yields in cultures treated with the NTC asMO were set at 100%.

consistent with observations on the mobility of the neurofilament heavy chain protein which has a predicted mol wt of ~100 kDa, but migrates on SDS-PAGE gels as a ~200 kDa polypeptide.

In order to determine the requirement of 46K and 32R for virus replication *in vitro*, viral titers were determined at 24 h p.i. by plaque assay. As shown in Fig. 2, viral titers were reduced by 77% after 46K knockdown and 81% after 32R knockdown. This result was confirmed by transmission electron microscopy. Cells treated with a control asMO showed hallmarks of a productive FV3 infection including chromatin condensation (consistent with the onset of apoptosis), assembly site formation, and progeny virions within paracrystalline arrays and scattered throughout the cytoplasm (Fig. 3, panel A). In contrast, although asMO-treated cells formed viral assembly sites and appeared to undergo apoptosis, events that are indicative of an ongoing infection, infected cells were markedly devoid of progeny virions (Fig. 3, compare panels B and C to panel A) indicating that both 46K and 32R are essential for FV3 replication *in vitro*.

3.2. siRNA-mediated silencing

As an alternative to asMO-mediated KD, we next sought to target FV3 gene expression using RNAi. Initially, we attempted to silence viral gene expression using siRNA pools (final concentration = 100 mM) containing two–three siRNA species and targeted to MCP, vPol-IIα, or DMT transcripts. However, we were unable to consistently demonstrate a reduction in the level of the targeted messages by either 1D SDS-PAGE or RT-PCR when a MOI of ~10 PFU/cell was used (data not shown). Since transfection with siGLO indicated that the majority of treated cells were successfully transfected, our failure to detect silencing was not due to the inability of the siRNA to enter target cells. Moreover, since others have reported successful siRNA-mediated silencing when using MOIs of one or lower, we reduced the MOI to ~1 PFU/cell and monitored silencing at 48 h p.i. (Dave et al., 2006; Yamauchi et al., 2008; Vigne et al., 2008; Falkenhagen et al., 2009). Preliminary experiments indicated that silencing occurred in FHM cells pre-treated with siRNA at this lower MOI (data not shown).

To determine which siRNAs were most effective in blocking virus replication, we next monitored the ability of individual siRNAs to block viral gene expression. We observed marked reductions in the levels of MCP, vPol-IIα, and DMT transcripts following treatment with each of the siRNAs assayed. Moreover, although all siRNAs inhibited FV3 gene expression, for each set there was one siRNA that was most effective and these were chosen for additional studies (Table 1; data not shown). To confirm the above result and determine whether siRNA-mediated silencing of FV3 gene expression is MOI-dependent, we treated FHM cells with anti-MCP-4 and 24 h later infected them with FV3 at MOIs ranging from 0.01 to 10 PFU/cell. Three sets of replicate cultures were examined: one to determine the level of mRNA silencing by qRT-PCR, a second for determining viral yield by plaque assay, and a third set to monitor virion assembly by transmission electron microscopy. To quantify the level of mRNA silencing, we performed qRT-PCR analysis on total RNA extracted from each culture and determined the relative levels of MCP, vPol-IIα, and DMT transcripts. The level of MCP transcripts, along with those for vPol-IIα and DMT, were not reduced in virus-infected cells treated with a control siRNA indicating that transfection with non-targeting RNA did not inhibit overall viral gene expression (data not shown). Likewise, little to no inhibition of MCP gene expression was observed at the two highest MOIs tested (1 and 10 PFU/cell; Fig. 4, panel A). However, when the MOI was reduced to ≤0.1 PFU/cell, a marked decrease in the level of gene expression was observed in cultures pretreated with anti-MCP-4 siRNA. At the lower MOIs, MCP gene expression was reduced by ~80% compared to levels seen in control treated cultures (Fig. 4, panel A). Surprisingly, along with the reduction in MCP transcripts, there was also a ~80% reduction in the expression levels of two additional non-targeted viral genes (Fig. 4, panels B and C). Because MCP, vPol-IIα, and DMT transcripts were not reduced by treatment with negative control siRNA, or when MOIs ≥ 1.0 PFU/cell were used, we suggest that reductions in vPol-IIα and DMT levels were not a result of "off targeting," but rather reflect the cumulative effect of siRNA-mediated silencing of MCP expression and the resulting inhibition of both the initial and subsequent rounds of FV3 replication. Since less than 10% of cells are infected at an MOI of 0.1 PFU/cell and less than 1% are infected at an MOI of 0.01 PFU/cell,

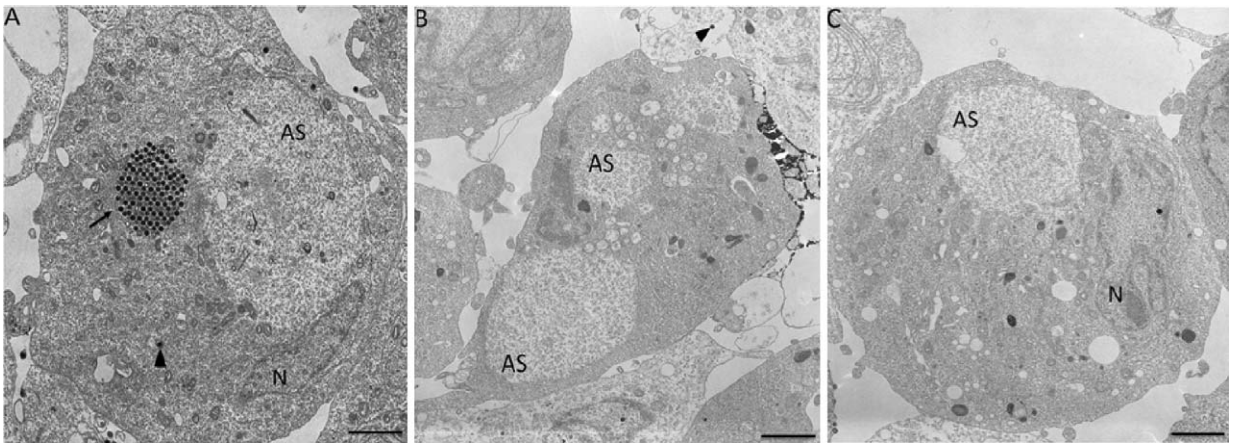

Fig. 3. Transmission electron microscopy of control, anti-46K, and anti-32R asMO treated FV3-infected FHM cells. FHM cells were treated with a non-targeting negative control (NTC), anti-46K, or anti-32R asMOs and 24 h later infected with FV3 (MOI = 20 PFU/cell). At 9 h p.i. cultures were fixed in 2% glutaraldehyde and processed for electron microscopy. Panel A: NTC-treated, FV3-infected FHM cells. Panel B: Anti-46K asMO-treated, FV3-infected FHM cells. Panel C: Anti-32R asMO-treated, FV3-infected FHM cells. N, nucleus; AS, assembly site; closed arrowhead indicate mature virions; arrow indicates a paracrystalline array. Scale bars represent 1.5 μm.

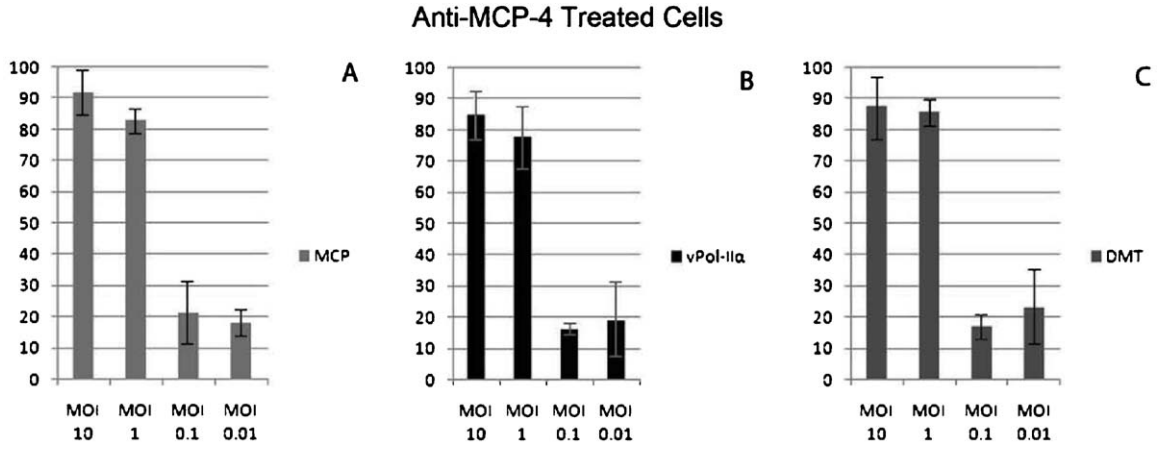

Fig. 4. Effect of multiplicity of infection on siRNA mediated silencing: qRT-PCR analysis. FHM cells were treated with a non-silencing control RNA or anti-MCP-4 siRNA and 24 h later infected at the MOIs shown. Total RNA was isolated at 48 h p.i. and message levels determined by qRT-PCR. The specific transcripts assayed are shown to the right of each panel, the percent gene expression relative to the non-silencing control is indicated along the left of each panel, and the MOI is listed on the *X*-axis. Numerical values for error bars were calculated to a 95% confidence interval based on three independent experiments with samples analyzed in triplicate.

infection of the complete monolayer likely requires two or more rounds of virus replication. Given that treatment with anti-MCP-4 siRNA likely inhibits virus replication in the few cells initially infected, markedly fewer virions will be available to initiate subsequent rounds of replication with the result that the level of total viral transcripts will be markedly depressed. Collectively, these results suggest that in the FV3 system, siRNA-mediated silencing is MOI dependent and is only seen at lower MOIs.

In an attempt to further confirm the effect of gene silencing on virus replication we assayed the resulting virus yields from both control and anti-MCP-4 siRNA treated cultures at ~48 h p.i. As shown in Fig. 5 anti-MCP-4 treatment had little effect on replication at MOIs ≥ 1.0 PFU/cell, i.e., cultures infected at an MOI of 1.0 and 10.0 PFU/cell produced yields that were ~96% and ~98% of those seen in control treated cultures infected at the same MOI. However, as the MOI was reduced to 0.1 and 0.01 PFU/cell the resulting virus yields were reduced to ~17% and ~16%, respectively, of those seen in control treated cultures (Fig. 5). These results further support the qRT-PCR findings and suggest that siRNA-mediated silencing is inversely related to the MOI. Lastly, we examined the effect of anti-MCP siRNA treatment by transmission electron microscopy. FV3-infected cells treated with a control siRNA showed abundant virion formation with virus particles present within assembly

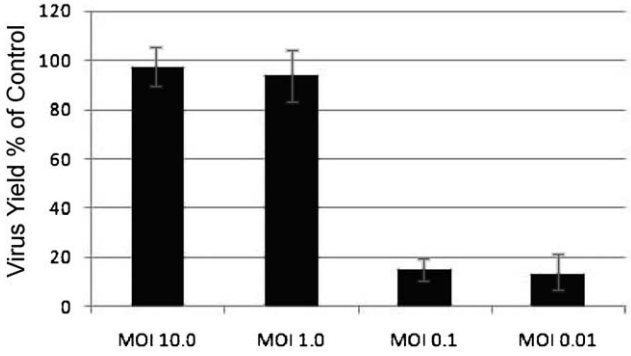

Fig. 5. Effect of multiplicity of infection on siRNA mediated silencing: Virus yield analysis. FHM cells were treated with a non-silencing control siRNA or a siRNA targeting the MCP (anti-MCP-4). Twenty-four hours after treatment, the cultures were infected at the indicated MOIs, and 48 h later the cultures were harvested and virus yields determined by plaque assay. Virus yields are expressed as a percentage of those achieved in control treated cultures. MOIs are shown on the *X*-axis and percent yield is shown along the *Y*-axis. Error bars were calculated to a 95% confidence interval based on three independent experiments with samples analyzed in duplicate. Virus yields were analyzed using a randomized block design ANOVA to assess differences in titers among treatment categories at a statistical significance level of $\alpha = 0.05$ (http://www.statsoft.com/textbook/anova-manova/).

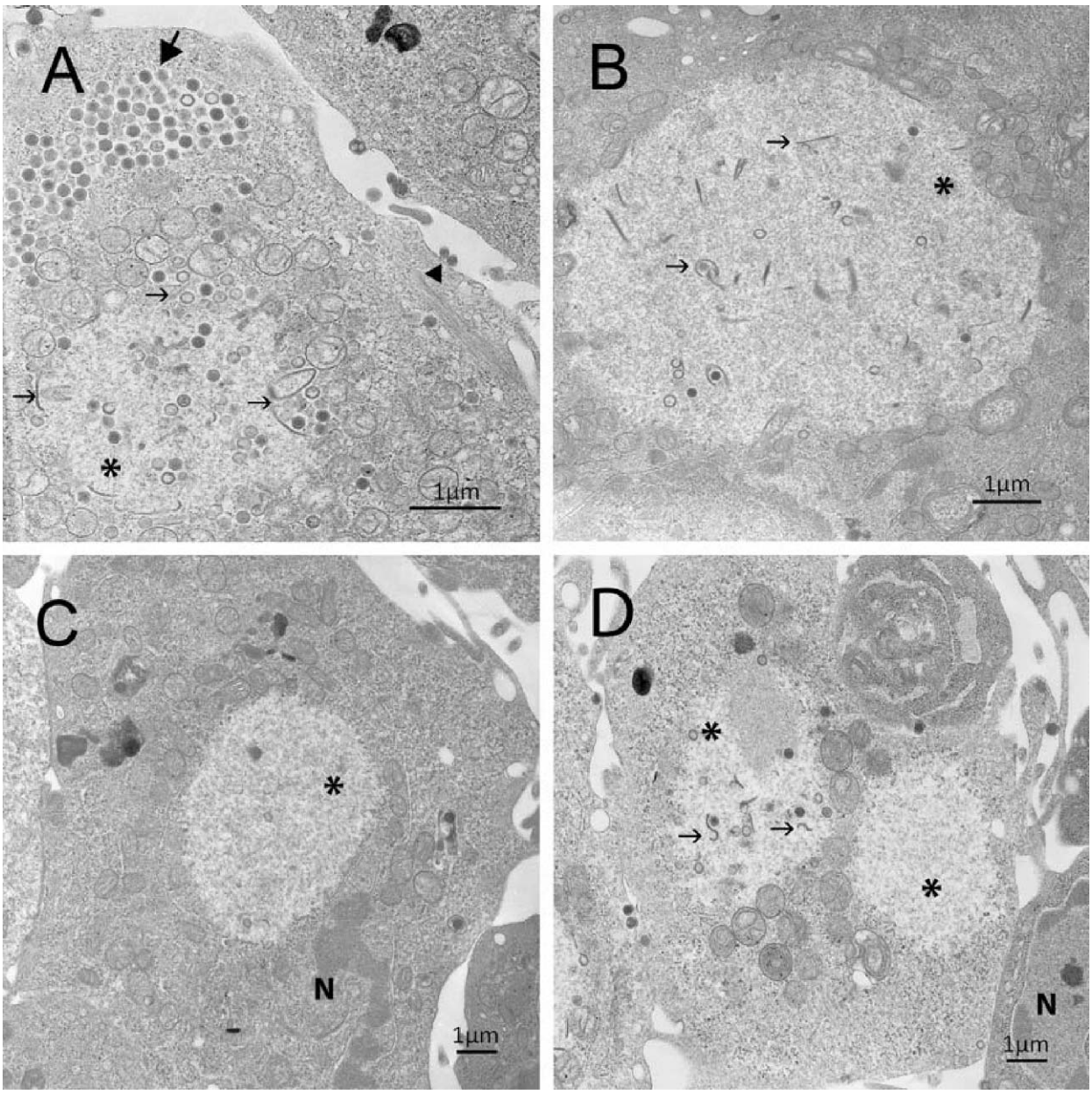

Fig. 6. Effect of siRNA treatment on FV3 replication: Transmission electron microscopy. FHM cells were treated with control, anti-MCP-4, anti- vPol-IIα-1, or anti-DMT-1 siRNAs, and infected with FV3-RFP at an MOI ~0.1 PFU/cell 24 h later. Cells were harvested at 48 h p.i., fixed, and processed for electron microscopy. Panel A was treated with a non-silencing control siRNA prior to infection; panels B, C, and D received prior treatment with anti-MCP-4, anti-vPol-IIα-1, or anti-DMT-1 siRNAs, respectively. N, nucleus; *, viral assembly sites; large arrows identify virions within paracrystalline arrays; small arrowheads identify budding virions; and slender arrows identify aberrant structures. Magnification: panel A – 10,000×; panel B – 7750×; panel C – 4646×; panel D – 4646×.

sites, paracrystalline arrays, and budding from the plasma membrane (Fig. 6A). In contrast, cells treated with anti-MCP-4 siRNA showed a marked reduction in virion formation and the presence of aberrant structures, reminiscent of the atypical elements seen in FV3-infected cells treated with an asMO targeted against the MCP (Fig. 6B, Sample et al., 2007). Collectively these results confirmed that anti-MCP-4 siRNA reduced MCP gene expression and resulted in a decrease in the synthesis of mature virus particles.

3.3. Silencing vPol-IIα expression

We next targeted vPol-IIα, a viral gene product previously linked to late gene transcription (Sample et al., 2007). qRT-PCR analysis demonstrated a >90% reduction in vPol-IIα message levels following treatment (Fig. 7, panel A). In addition, as seen with a siRNA directed against the MCP, there was a drop in non-targeted MCP and DMT transcript levels. This result was not unexpected since both MCP and DMT are late genes and require vPol-IIα for their transcription (Sample et al., 2007; Majji et al., 2009). However, given the results of previous treatment with an anti-MCP siRNA, the reduction in MCP and DMT levels also likely reflects the effect of siRNA on initial and subsequent rounds of virus replication. Consistent with reductions in viral transcripts, virus yields declined >90% compared to control treated cultures, and transmission electron microscopy (Fig. 6C) showed a marked reduction in virion formation and assembly sites that were completely devoid of viral intermediates.

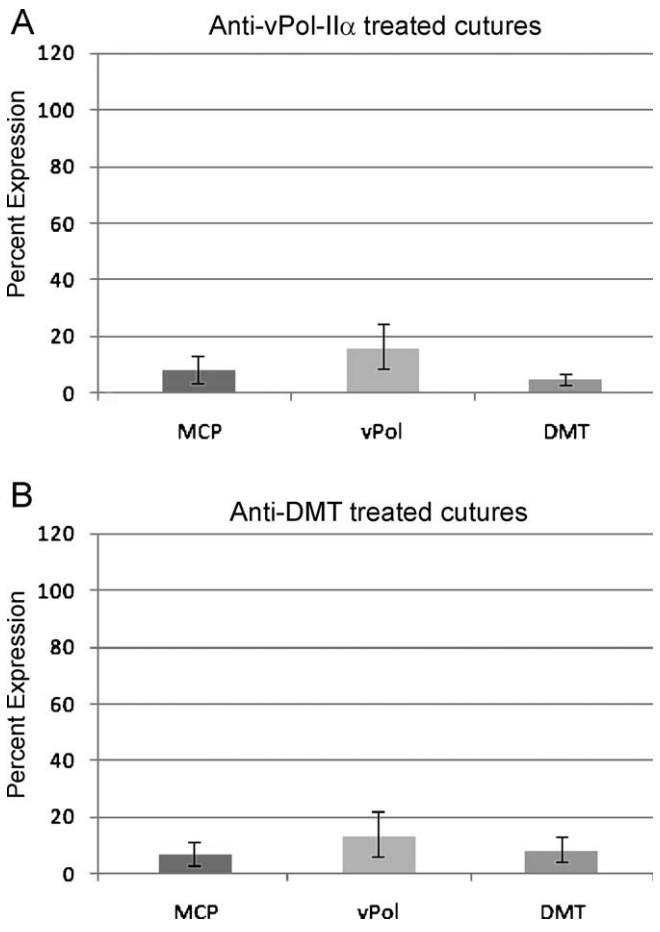

Fig. 7. FV3 gene expression following treatment with anti-vPol-IIα-1 and anti-DMT-1 siRNAs: qRT-PCR. FHM cells were treated with a non-silencing control and anti-vPol-IIα-1 (panel A) or anti-DMT-1 (panel B) siRNAs. Cells were infected at an MOI ~0.1 PFU/cell at 24 h post treatment. Total RNA was isolated at 48 h p.i., and message levels determined by qRT-PCR. The percent gene expression and the specific transcripts monitored are shown along the left and bottom edges, respectively. Levels of expression have been normalized to the expression of FHM 18S rRNA. Numerical values for error bars were calculated to a 95% confidence interval based on three independent experiments with samples analyzed in triplicate.

3.4. Silencing DNA methyltransferase expression

We next targeted the FV3 DMT gene to determine if it was essential for virus replication *in vitro*. Previous work indicated that the virus-encoded DMT was responsible for viral DNA methylation and that inhibition of DMTase activity resulted in a 100-fold drop in virus titers (Goorha et al., 1984; Essani et al., 1987). However, since the former study utilized 5′ azacytidine, a general inhibitor of DNA methylation, rather than an inhibitor specific for the virus-encoded DMT, we wished to determine the impact of targeted knock down on virus replication. qRT-PCR analysis showed a dramatic drop in DMT message levels within anti-DMT-1 siRNA treated cells compared to control-treated cells (Fig. 7, panel B). In addition, there was also a parallel drop in the levels of MCP and vPol-IIα transcripts most likely reflecting the cumulative effect of inhibiting virus replication and not due to off targeting or a direct effect of DMT silencing on heterologous viral gene expression. Consistent with the reduction in viral messages, virus yields were reduced > 95%. Transmission electron microscopy confirmed both findings and showed a marked reduction in virion formation in anti-DMT-1 treated cultures (Fig. 6D). These results were similar to earlier results from cells treated with 5′ azycytidine (Goorha et al., 1984) and indicate that DMT is an essential gene product.

4. Discussion

Previous studies have shown that asMOs and siRNAs targeted to specific transcripts can be used to elucidate FV3 gene function (Xie et al., 2005; Sample et al., 2007; Whitley et al., 2010). Moreover, asMOs have been used to inhibit translation in variety of cellular and viral systems (Sumanas and Ekker, 2001; Munshi et al., 2002; Zhang et al., 2007; Vagnozzi et al., 2007; Stein et al., 2008; Lupfer et al., 2008). For example, asMOs-targeting the 5′ terminal region and the 3′ region responsible for cyclization of Dengue virus genomic RNA inhibited replication 1000-fold *in vitro*. Moreover, intraperitoneal injection of these asMOs increased survival of Dengue virus-infected mice by 8 days suggesting a therapeutic role for these agents (Stein et al., 2008). In other studies, asMOs targeting transcriptional regulators of Kaposi's sarcoma-associated herpesvirus inhibited viral gene expression and suppressed replication (Zhang et al., 2007), and intranasal administration of asMOs targeted to conserved regions within the nucleoprotein and the PB1 polymerase protein protected mice from influenza A virus (Lupfer et al., 2008). Likewise, siRNAs have been shown to silence gene expression in a number of viruses including hepatitis A and B viruses, rotavirus, measles virus, retroviruses, and respiratory syncytial virus (Hu et al., 2002; Zhou et al., 2002; Arias et al., 2004; Randall and Rice, 2004; Hu et al., 2005; Lu et al., 2005; Neuman et al., 2005; Jia et al., 2006; Kusov et al., 2006; Guang et al., 2010; Zhang et al., 2010; Zhiqiang et al., 2010).

4.1. asMO knock down of 46K and 32R proteins

Initially, we sought to determine the roles of the FV3 46K and 32R proteins using asMOs. We showed that knock down of these two proteins resulted in the marked inhibition of viral replication. However, unlike knock down of vPol-IIα that was characterized by a marked reduction in late viral gene expression, knock down of 46K and 32R only affected the target proteins. Furthermore, although the data indicated that both 46K and 32R were essential for virus replication *in vitro*, the precise roles of 46K and 32R remain to be determined. In the former case, FV3 46K, a viral gene with limited sequence identity to T4 RNA ligase, could act as a repair enzyme to combat host antiviral responses. In *Escherichia coli* there is evidence that bacterial damage to lysine-tRNA limits phage replication (Amitsur et al., 1987). Accordingly, bacteriophage T4 RNA ligase has been implicated in the repair of damaged tRNA molecules and the maintenance of phage replication within *E. coli*. Perhaps, the T4 RNA ligase-like activity of 46K repairs tRNAs damaged either as a result of a host-induced antiviral response or as a consequence of the virus-induced degradation of cellular RNA (reviewed in Chinchar et al., 2009).

BLAST analysis identified 32R as a protein with marked amino acid sequence identity with the human neurofilament heavy chain (NFH) protein. NFH is member of the intermediate filament family of proteins and, along with light and medium chains, forms neurofilaments. The main role of neurofilaments is to increase the axonal caliber of myelinated axons and, in doing so, their conduction velocity. In addition neurofilaments contribute to the dynamic properties of the axonal cytoskeleton during neuronal differentiation, axon outgrowth, regeneration and guidance (Lee and Cleveland, 1996; Perrot et al., 2008). The NFH protein is characterized by the presence of multiple lysine–serine–proline (KSP) repeats which likely serve as sites for serine phosphorylation (Fig. 8A). This high level of phosphorylation, coupled with a high percentage of acidic amino acids, may be responsible for the anomalous migration of NFH on SDS-polyacrylamide gels, i.e., although NFH has a predicted mol wt of ~100,000, it migrates on SDS-polyacrylamide gels as a protein of nearly 200,000 mol wt. Like NFH, the 32R gene product displays multiple KSP repeats embedded

Neurofilament heavy (NFH) polypeptide (*H.sapiens*)

MMSFGGADALLGAPFAPLHGGGSLHYALARKGGAGGTRSAAGSSSGFH
SWTRTSVSSVSASPSRFRGAGAASSTDSLDTLSNGPEGCMVAVATSRS
EKEQLQALNDRFAGYIDKVRQLEAVRQRLDDEARQREEAEAAARALARF
AQEAEAARVDLQKKAQALQEECGYLRRHHQEEVGELLGQIQGSGAAQA
QMQAETRDALKCDVTALREIRAQLEGHAVQSTLQSEEWFRVRLDRLSEA
AKVNTDAMRSAQEEITEYRRQLQARTTELEALKSTKDSLERQRSELEDRH
QADISSYQEAIQQLDAELRNTRWEMAAQLREYQDLLNVKMALDIEIAAYR
KLLEGEECRIGFPIPFSLPEGLPKIPSVSTHIKVKSEEKIKVVEKSEKETVIV

EEQTEETQVTEEVT**EEEEE**KEAK**EEE**GK**EEE**GG**EEEEE**AEGG**EEE**T**KSP**PA

EEAASPEKEA**KSP**VKEEA**KSP**AEA**KSP**EKEEA**KSP**AEV**KSP**EKA**KSP**AK

EEA**KSP**PEA**KSP**EKEEA**KSP**AEV**KSP**EKA**KSP**AKEEA**KSP**AEA**KSP**EKA

KSPVKEEA**KSP**AEA**KSP**VKEEA**KSP**AEV**KSP**EKA**KSP**TKEEA**KSP**EKA**K**

SPEKEEA**KSP**EKA**KSP**VKAEA**KSP**EKA**KSP**VKAEA**KSP**EKA**KSP**VKEEA

KSPEKA**KSP**VKEEA**KSP**EKA**KSP**VKEEAKTPEKA**KSP**VKEEA**KSP**EKA**K**

SPEKAKTLDV**KSP**EAKTPAKEEARSPADKFPEKA**KSP**VKEEV**KSP**EKA**K**

SPLKEDAKAPEKEIPKKEEV**KSP**VK**EEE**KPQEVKVKEPPKKA**EEE**KAPAT

PKTEEKKDSKKEEAPKKEAPKPKVEEKKEPAVEKPKESKVEAKKEEAEDK
KKVPTPEKEAPAKVEVKEDAKPKEKTEVAKKEPDDAKAKEPSKPAEKKEA
APEKKDTKEEKAKKPEEKPKTEAKAKEDDKTLSKEPSKPKAEKAEKSSST
KQKDSKPPEAATEDKAAKGK

Repeats motifs within the middle third of NFH:

(KSP [N]$_5$ K)$_{15}$ and (KSP [N]$_3$ K)$_{18}$

FV3 ORF 32R

MVTVTELRATAKNLGIRGYSTMRKAELEEAIRDHGRVSEARVASPRRSPARSPR**KSP**A

GR**KSP**S**KSP**AGR**KSP**S**KSP**AGR**KSP**S**KSP**AGR**KSP**S**KSP**AGR**KSP**

S**KSP**VR**KSP**S**KSP**VR**KSP**R**KSP**AAKLQAGDRPASMNICKNLPKQRLVDIATEMGIDLN

RESDGKPKTKDQLCADIMGGAGR**KSP**R**KSP**SRSPVR**KSP**SRSPVR**KSP**VRSPR**KSP**

VRVPSPVRSPVKEKTPVRSPARSEDAGSDLAPRPRRGKAVRL**DYDEDDD**YSYGASTD

NLFSGNKEIPFPTRKRRTRKPEKVFVDVRSPHTLTDS**EDEDD**MVEVPELEDKEITMPG

VLSPYSDEIVERGYVSQGGADYINYIYRTEYALESDESFARGARPKTNKRDSDRAVRE

AAAAAAIARALDRRSQSGNDEPAVRRRSAPTDSSRESRRDREPQRDIAEPQRDIAEPQ

RDIAEPQRDIAEPRKVRFREAGSADVRVFERDEPKEYGRVPVRPPLFMPAGEPLQPLK

FRPKTPKIDDTIHRAQMVLPSKPSQKETDNYYKQFAGEAVRPSEPVQWDKDDQVLYH

KVPAWDDSSYAAAVSAWPMSVDPKQAESVFAEFEQLSAQDSDLIKVRKSIMKALGY

NH_2 – [N]$_{54}$ [AGRKSPSKSP]$_6$ [VRKSPSKSP]$_2$…[AGRKSPRKSP] [N]$_4$
[VRKSPSRSP]$_2$…-COOH

Fig. 8. Comparison of the amino acid sequences of NFH and 32R. Panel A, NFH: KSP repeats within the human NFH protein are indicated in boldface type and the central region containing these repeats is highlighted. Several areas containing stretches of acidic amino acids are indicated by double underlining. Panel B, 32R: Conserved and degenerate AGRKSPSKSP repeats are underlined and KSP motifs are displayed in boldface type; conserved and degenerate VRKSPSKSP repeats are indicated by double underlining. Two stretches of acidic amino acids are indicated by wavy underlining and boldface type. GenBank accession numbers: FV3 ORF 32R, AY548484 and human NFH, NP_066554.

within the context of a larger repeat structure (Fig. 8B). Inspection of the 32R sequence shows six tandem AGR**KSP**S**KSP** repeats followed by tandem VR**KSP**S**KSP** repeats. Furthermore, additional KSP repeats and several less-conserved versions of the two above motifs are found within the N-terminal portion of the protein. Based on the presence of multiple KSP sequences, it is possible that, as with NFH, serine residues within 32R are highly phosphorylated. At this time it is not clear whether a host or virus-encoded enzyme is involved in this process. However, FV3 and other iridoviruses encode a putative serine–threonine protein kinase (FV3 ORF 57R) that may be responsible for this activity (Tan et al., 2004). Aside from the putative high level of phosphorylation, there are two runs of five acidic amino

acids (DEDDD and EDEDD). These acidic patches, coupled with the high degree of phosphorylation, could explain 32R's anomalous migration (>100 kDa vs. the expected 70 kDa) on SDS-PAGE gels.

Earlier work showed that the cytoskeletal framework of the host cell is markedly rearranged following FV3 infection (Murti et al., 1985). Electron microscopic analysis showed that intermediate filaments surround viral assembly sites and may serve to anchor them within the cell or exclude large cellular organelles. Moreover, vimentin, another class of intermediate filament protein, is phosphorylated in FV3 infected cells (Chen et al., 1986) and FV3 proteins appear to be synthesized on intermediate filament-bound polyribosomes (Murti and Goorha, 1989). Perhaps, in addition to utilizing host intermediate filaments, FV3 ORF 32R may also play a role in these processes.

Lastly, although 32R is not required for assembly site formation (Fig. 3C), it may play a role in the release of viral particles from infected cells, or function in some unknown aspect of intracellular trafficking. In view of the above, experiments are planned to determine if 32R contains phosphoserine residues, and to ascertain if inhibition of phosphorylation, either using PD98059, an inhibitor of MAP kinases that targets KSP motifs (Veeranna et al., 1998), or an asMO targeted to the putative FV3 serine/threonine kinase (FV3 ORF 57R), adversely affects viral replication.

4.2. siRNA

The abovementioned results indicate that siRNAs are also suitable tools for silencing the expression of ranavirus genes and determining whether a given viral gene is essential for virus replication. However, because siRNA silencing is only seen at low MOIs, it may be more difficult to infer gene function since at the time of assay, generally 48 h p.i., the levels of all viral genes are reduced. Clearly, we will need to improve the sensitivity of our qRT-PCR assay by detecting viral gene expression in those few cells initially infected at low MOIs if we wish to ascertain whether siRNA- mediated KD plays a direct or indirect role in the expression of other viral genes.

The results shown here indicate that the ability of a given siRNA to silence FV3 gene expression is inversely related to the MOI. At multiplicities of infection greater than 1 PFU/cell siRNA-mediated inhibition was not seen, whereas at lower MOIs silencing was detected. The inability to achieve silencing at high MOIs may be due to several factors. In the first place, FV3, like several other plant and animal viruses, may encode one or more proteins that block an RNAi response (Lichner et al., 2003; Li et al., 2004; Soldan et al., 2005; Sullivan and Ganem, 2005; Van Rij and Andino, 2008). For example, the E3L protein of vaccinia virus (genus *Orthopoxvirus*, family Poxviridae) has been shown to sequester double-stranded RNA (dsRNA) and thereby prevent activation of protein kinase R and thus maintain viral protein synthesis in infected cells (Chang and Jacobs, 1993; Langland and Jacobs, 2002). In addition, by sequestering dsRNA, E3L may also prevent dsRNA's interaction with RIG-I, MDA-5, or TLR-3 and block the induction of interferon (Hiscott, 2004; Levy and Marie, 2004). Moreover, by binding and/or sequestering viral dsRNA, E3L may also block the cleavage and processing of large dsRNA molecules and thereby prevent the generation of siRNAs. Lastly, E3L may bind exogenously introduced siRNA and inhibit siRNA-mediated silencing.

Although FV3 does not contain a protein homologous to E3L, it encodes a putative ribonuclease III-like protein (ORF 80R), and thus shares limited homology to other proteins that bind and degrade dsRNA. We speculate that 80R may possess a non-traditional dsRNA binding domain that allows it to bind and sequester dsRNA and inhibit RNAi. If so, infection at high MOIs may result in either increased synthesis of 80R or the release of elevated levels of virion-associated 80R and result in the inhibition of siRNA silencing. Alternatively, FV3 infection may simply overwhelm the RNAi pathway. The RNA-induced silencing complex is believed to be present within the cell in tightly regulated, limited quantities (Vickers et al., 2007). Therefore, the marked inhibition of host gene expression observed following FV3 infection could result in reduced levels of the RNA induced silencing complex at a time when demand for its function are increasing (Schmitter et al., 2006; Peters and Meister, 2007). As a consequence, the remaining complexes cannot silence the increasing levels of viral transcripts.

Taken together, the results obtained following targeting MCP, vPol-IIα, and DMT by siRNA are comparable to those seen earlier following asMO-mediated knock down of MCP and vPol-IIα expression, or inhibition of DMT function by 5-azacytidine (Sample et al., 2007; Goorha et al., 1984). Moreover, the success of siRNA-mediated KD demonstrates the utility of this approach for determining whether a given viral gene product is essential for replication *in vitro*.

The complementary asMO and siRNA approaches described above will allow us to determine if individual FV3 genes are essential for replication *in vitro*, and, in some cases, to infer gene function following changes in phenotype. Knock down mediated by asMOs is suitable for proteins that can be readily visualized by 1D or 2D electrophoresis (e.g., MCP) or for which antibodies suitable for Western blot analysis are available (e.g., 53R). Alternatively, because siRNA-mediated knock down can be monitored by RT-PCR, siRNAs are useful for those genes whose cognate proteins are present in low amounts, co-migrate with more abundant products, and for which antibodies have not yet been generated. Moreover, because siRNAs can potentially target multiple sites within a message, whereas asMOs are limited to regions upstream or immediately surrounding the initiation codon, RNAi can be employed against targets for which effective asMOs cannot be designed. This is especially important for ranaviruses where most 5′ non-translated regions have not yet been mapped and those that have tend to be very short (e.g., as little at 8–15 nts) and AU-rich. Although asMOs and siRNAs will allow us to determine whether a specific FV3 gene is essential for replication in a given cell type *in vitro*, extension of these studies to whole animals, e.g., *Xenopus* (Gantress et al., 2003), will require advances in *in vivo* delivery systems and/or development of effective knock out strategies for iridoviruses. While progress in the former is encouraging, recent work suggests that ranavirus genes can be efficiently knocked out and deletion mutants isolated by homologous recombination using a selectable marker flanked by DNA surrounding the gene of interest (James Jancovich, PhD dissertation, Arizona State University). Taken together the combination of knock down and knock out approaches will allow us to identify viral virulence and immune evasion genes and to determine which components of the amphibian immune response play critical roles in anti-viral immunity.

Acknowledgements

This work was partially supported by NSF Award No. IOS-07-42711; stipend support (for RCS.) was provided by the School of Graduate Studies in the Health Sciences, University of Mississippi Medical Center. AsMO experiments were carried out by DSW and siRNA work by RCS; both students contributed equally to this work.

References

Alcami, A., Koszinowski, U.H., 2000. Viral mechanisms of immune evasion. Mol. Med. Today 6, 365–373.

Altschul, S.F., Madden, T.L., Schaffer, A.A., Zhang, J., Zhang, Z., Miller, W., Lipman, D.J., 1997. Gapped BLAST and PSI-BLAST: a new generation of proein datavbaase search programs. Nuc. Acids Res. 25, 3389–3402.

Amitsur, M., Levitz, R., Kaufman, G., 1987. Bacteriophage T4 anticodon nuclease, polynucleotide kinase, and RNA ligase reprocesses the host lysine tRNA. EMBO J. 6, 2499–2503.

Arias, C., Dector, M., Segovia, L., Lopez, T., Camacho, M., Isa, P., Espinosa, R., Lopez, S., 2004. RNA silencing of rotavirus gene expression. Virus Res. 102, 43–51.
Appasani, K., 2011. RNA Interference Technology. Cambridge University Press, Cambridge, UK.
Chang, H., Jacobs, B., 1993. Identification of a conserved motif that is necessary for binding of the vaccinia virus E3L gene products to double-stranded RNA. Virology 194, 537–547.
Chen, M., Goorha, R., Murti, K.G., 1986. Interaction of frog virus 3 with the cytomatrix. IV. Phosphorylation of vimentin precedes the reorganization of intermediate filaments around the virus assembly sites. J. Gen. Virol. 67, 915–922.
Chinchar, V.G., Hyatt, A., Miyazaki, T., Williams, T., 2009. Family *Iridoviridae*: poor viral relations no longer. Curr. Top. Microbiol. Immunol. 328, 123–170.
Cunningham, A.A., Langton, T.E.S., Bennett, P.M., Lewin, J.F., Drury, S.E.N., Gough, R.E., MacGregor, S.K., 1996. Pathological and microbiological findings from incidents of unusually mortality of the common frog (*Rana temporaria*). Philos. Trans. R. Soc. Lond. B 351, 1539–1557.
Dave, R., McGettigan, J., Qureshi, T., Schnell, M., Nunnari, G., Pomerantz, R., 2006. siRNA targeting Vaccinia virus double-stranded RNA binding protein [E3L] exerts potent antiviral effects. Virology 348, 489–497.
Duffus, A.L.J., Pauli, B.D., Wozney, K., Brunnetti, C.R., Berrill, M., 2008. Frog virus 3-like infections in aquatic amphibian communities. J Wildl. Dis. 44, 109–120.
Eaton, H.E., Metcalf, J., Penny, E., Tcherepanov, V., Upton, C., Brunetti, C.R., 2007. Comparative genomic analysis of the family Iridoviridae: re-annotating and defining the core set of iridovirus genes. Virol J. 4, 11.
Ekker, S.C., Larson, J.D., 2001. Morphant technology in model developmental systems. Genesis 30, 89–93.
Essani, K., Goorha, R., Granoff, A., 1987. Mutation in a DNA binding protein reveals an association between DNA methyltransferase activity and a 26 kDa polypeptide in FV3-infected cells. Virology 161, 211–217.
Falkenhagen, A., Heinrich, J., Moelling, K., 2009. Short hairpin-loop-structured oligodeoxynucleotides reduce HSV-1 replication. Virol. J. 6, 43–49.
Gantress, J., Maniero, G.D., Cohen, N., Robert, J., 2003. Development and characterization of a model system to study amphibian immune responses to iridoviruses. Virology 311, 254–262.
Goorha, R., Granoff, A., Willis, D.B., Murti, K.G., 1984. The role of DNA methylation in virus replication: Inhibition of frog virus 3 replication by 5' azacytidine. Virology 138, 94–102.
Granoff, A., Came, P., Rafferty, K., 1965. The isolation and properties of viruses from *Rana pipiens*: their possible relationship to the renal adenocarcinoma of the leopard frog. Ann. N.Y. Acad. Sci. 126, 237–255.
Gray, M.J., Miller, D.L., Hoverman, J.T., 2009. Ecology and pathology of amphibian ranaviruses. Dis. Aquat. Org. 87, 243–266.
Green, D.E., Converse, K.A., Schrader, A.K., 2002. Epizootiology of sixty-four amphibian morbidity and mortality events in the USA, 1996–2001. Ann. N.Y. Acad. Sci. 969, 323–339.
Greer, A.L., Berrill, M., Wilson, P.J., 2005. Five amphibian mortality events associated with ranavirus infection in south central Ontario, Canada. Dis. Aquat. Org. 67, 9–14.
Guang, S., Bochner, A.F., Burkhart, K.B., Burton, N., Pavelec, D.M., Kennedy, S., 2010. Small regulatory RNAs inhibit RNA polymerase II during the elongation phase of transcription. Nature 465 (7301), 1097–1101.
Guselnikov, S.V., Ramanayake, T., Erilova, A.Y., Mechetina, L.V., Najakshin, A.M., Robert, R., Taranin, A.V., 2008. The Xenopus FcR family demonstrates continually high diversification of paired receptors in vertebrates evolution. BMC Evolutionary Biology 8, 148.
He, J.G., Lu, L., Deng, M., He, H.H., Weng, S.P., Wang, X.H., Zhou, S.Y., Long, Q.X., Wang, X.Z., Chan, S.M., 2002. Sequence analysis of the complete genome of an iridovirus isolated from the tiger frog. Virology 292, 185–197.
Hiscott, J., 2004. Another detour on the toll road to the interferon antiviral response. Nat. Struct. Mol. Biol. 11, 1028–1030.
Hu, L., Wang, Z., Hu, C., Liu, X., Yao, L., Li, W., Qi, Y., 2005. Inhibition of measles virus multiplication in cell culture by RNA interference. Acta Virol. 49, 227–234.
Hu, W., Myers, C., Kilzer, J., Pfaff, S., Bushman, F., 2002. Inhibition of retroviral pathogenesis by RNA interference. Curr. Biol. 12, 1301–1311.
Huang, Y., Huang, X., Liu, H., Gong, J., Ouyang, Z., Cui, H., Cao, J., Zhao, Y., Wang, X., Jiang, Y., Qin, Q., 2009. Complete sequence determination of a novel reptile iridovirus isolated from soft-shelled turtle and evolutionary analysis of *Iridoviridae*. BMC Genomics 10, 224.
Jancovich, J.K., Davidson, E.W., Morado, J.F., Jacobs, B.L., Collins, J.P., 1997. Isolation of a lethal virus from the endangered tiger salamander *Ambystoma tigrinum stebbinsi*. Dis. Aquat. Org. 31, 161–167.
Jancovich, J.K., Mao, J., Chinchar, V.G., Wyatt, C., Case, S.T., Kumar, S., Valente, G., Subramanian, S., Davidson, E.W., Collins, J.P., Jacobs, BL, 2003. Genomic sequence of a ranavirus (family Iridoviridae) associated with salamander mortalities in North America. Virology 316, 90–103.
Jensen, B.B., Ersboll, A.K., Ariel, E., 2009. Susceptibility of pike *Esox lucius* to a panel of ranavirus isolates. Dis. Aquat. Org. 83, 169–179.
Jia, F., Zhang, Y., Liu, C., 2006. A retrovirus-based system to stably silence hepatitis B virus genes by RNA interference. Biotechnol. Lett. 28, 1679–1685.
Johnston, J.B., McFadden, G., 2003. Poxvirus immunomodulatory strategies: current perspectives. J. Virol. 77, 6093–6100.
Kusov, Y., Kanda, T., Palmenberg, A., Sgro, J., Gauss-Müller, V., 2006. Silencing of hepatitis A virus infection by small interfering RNAs. J. Virol. 80, 5599–5610.
Laemmli, U.K., 1970. Cleavage of structural proteins during assembly of the head of bacteriophage T4. Nature 227, 680–685.
Langland, J., Jacobs, B., 2002. The Role of the PKR-Inhibitory genes, E3L and K3L, in determining Vaccinia virus host range. Virology 299, 133–141.
Lee, M.K., Cleveland, D.W., 1996. Neuronal intermediate filaments. Ann. Rev. Neurosci. 19, 187–217.
Levy, D.E., Marie, I., 2004. RIGging an antiviral defense – it's in the CARDs. Nat. Immunol. 5, 699–701.
Li, W., Li, H., Lu, R., Li, F., Dus, M., Atkinson, P., Brydon, E., Johnson, K., Garcia-Sastre, A., Ball, L., Palese, P., 2004. Interferon antagonist proteins of influenza and vaccinia viruses are suppressors of RNA silencing. Proc. Natl. Acad. Sci. U.S.A. 101, 1350–1355.
Lichner, Z., Silhavy, D., Burgyan, J., 2003. Double-stranded RNA-binding proteins could suppress RNA interference-mediated antiviral defences. J. Gen. Virol. 84, 975–980.
Litman, G.W., Rast, J.P., Fugmann, S.D., 2010. The origins of vertebrate adaptive immunity. Nat. Rev. Immunol. 10, 543–553.
Livak, K.J., Schmittgen, T.D., 2001. Analysis of relative gene expression data using real-time PCR and the 2 (-delta delta C (T)) method. Methods 25, 402–408.
Long, S., Wilson, M., Bengten, E., Bryan, L., Clem, L.W., Miller, N.W., Chinchar, V.G., 2004. Identification of a cDNA encoding channel catfish interferon. Dev. Comp. Immunol. 28, 97–111.
Lu, R., Maduro, M., Li, F., Li, H., Broitman-Maduro, G., Li, W., Ding, S., 2005. Animal virus replication and RNAi-mediated antiviral silencing in *Caenorhabditis elegans*. Nature 436, 1040–1043.
Lupfer, C., Stein, D., Mourich, D., Tepper, S., Iversen, P., Pastey, M., 2008. Inhibition of influenza A H3N8 virus infections in mice by morpholino oligomers. Arch. Virol. 153, 929–937.
Majji, S., Thodima, V., Sample, R., Whitley, D., Deng, Y., Mao, J., Chinchar, V.G., 2009. Temporal expression of frog virus 3 (family *Iridoviridae*) genes. Virology 391, 293–303.
Meister, G., Tuschl, T., 2004. Mechanisms of gene silencing by double-stranded RNA. Nature 431, 343–349.
Morales, H.D., Abramowitz, L., Gertz, J., Sowa, J., Vogel, A., Robert, J., 2010. Innate immune responses and permissiveness to ranavirus infection of peritoneal leukocytes in the frog *Xenopus laevis*. J. Virol. 84, 4912–4922.
Munshi, C.B., Graeff, R., Lee, H.C., 2002. Evidence for a causal role of CD38 expression in granulocytic differentiation of human HL-60 cells. J. Biol. Chem. 277, 49453–49458.
Murti, K.G., Goorha, R., Chen, M., 1985. Interaction of frog virus 3 with the cytoskeleton. Curr. Top. Microbiol. Immunol. 116, 107–131.
Murti, K.G., Goorha, R., 1989. Synthesis of FV3 proteins occurs on intermediate filament-bound polyribosomes. Biol. Cell 65, 205–214.
Neuman, B., Stein, D., Kroeker, A., Churchill, M., Kim, A., Kuhn, P., Dawson, P., Moulton, H., Bestwick, R., Iversen, P., Buchmeier, M., 2005. Inhibition, escape, and attenuated growth of severe acute respiratory syndrome coronavirus treated with antisense morpholino oligomers. J. Virol. 79, 9665–9676.
Perrot, R., Berges, R., Bocquet, A., Eyer, J., 2008. Review of the multiple aspects of neurofilament functions, and their possible contribution to neurodegeneration. Mol. Neurobiol. 38, 27–65.
Peters, L., Meister, G., 2007. Argonaute proteins: mediators of RNA silencing. Mol. Cell 26, 611–623.
Randall, G., Rice, C., 2004. Interfering with hepatitis C virus RNA replication. Virus Res. 102, 19–25.
Sample, R.C., Bryan, L., Long, S., Majji, S., Hoskins, G., Sinning, A., Chinchar, V.G., 2007. Inhibition of protein synthesis and viral replication by antisense morpholino oligonucleotides targeted to the major capsid protein, 18 kDa immediate-early protein, and viral homolog of RNA polymerase II. Virology 358, 311–320.
Schmitter, D., Filkowski, J., Sewer, A., Pillai, R., Oakeley, E., Zavolan, M., Svoboda, P., Filipowicz, W., 2006. Effects of Dicer and Argonaute down-regulation on mRNA levels in human HEK293 cells. Nucleic Acids Res. 34, 4801–4815.
Soldan, S., Plassmeyer, L., Matukonis, K., Gonzalez-Scarano, F., 2005. La Crosse virus nonstructural protein NSs counteracts the effects of short interfering RNA. J. Virol. 79, 234–244.
Song, W.J., Qin, Q.W., Qiu, J., Huang, C.H., Wang, F., Hew, C.L., 2004. Functional genomics analysis of Singapore grouper iridovirus: complete sequence determination and proteomic analysis. J. Virol. 78, 12576–12590.
Stafford, J.L., Bengten, E., DuPasquier, L., Miller, N.W., Wilson, M., 2007. Channel catfish leukocyte immune-type receptors contain a putative MHC class I binding site. Immunogenetics 59, 77–91.
Stein, D.A., Huang, C.Y.H., Silengo, S., Amantana, A., Crumley, S., Blouch, R.E., Iversen, P.L., Kinney, R.M., 2008. Treatment of AG129 mice with antisense morpholino oligomers increases survival time following challenge with dengue 2 virus. J. Antimicrob. Chemother. 62, 555–565.
Sullivan, C., Ganem, D., 2005. A virus-encoded inhibitor that blocks RNA interference in mammalian cells. J. Virol. 79, 7371–7379.
Sumanas, S., Ekker, S., 2001. Xenopus frizzled-7 morphant displays defects in dorsoventral patterning and convergent extension movements during gastrulation. Genesis 30, 119–122.
Tan, W.G.H., Barkman, T.J., Chinchar, V.G., Essani, K., 2004. Comparative genomic analyses of frog virus 3, type species of the genus *Ranavirus* (family *Iridoviridae*). Virology 323, 70–84.
Tidona, C.A., Darai, G., 1997. The complete DNA sequence of lymphocystis disease virus. Virology 230, 207–216.
Tsai, C.T., Ting, J.W., Wu, M.H., Wu, M.F., Guo, I.C., Chang, C.Y., 2005. Complete genome sequence of the grouper iridovirus and comparsion of genomic organization with those of other iridoviruses. J. Virol. 79, 2010–2023.

Vagnozzi, A., Stein, D., Iversen, A., Rieder, E., 2007. Inhibition of foot-and-mouth disease virus infections in cell cultures with antisense morpholino oligomers. J. Virol. 91, 11669–11680.

Van Rij, R., Andino, R., 2008. The complex interactions of viruses and the RNAi machinery: a driving force in viral evolution. In: Origin and Evolution of Viruses, 2nd ed, pp. 161–181.

Veeranna, Amin, N.D., Ahn, N.G., Jaffe, H., Winters, C.A., Grant, P., Pant, H.C., 1998. Mitogen-activated protein kinases (Erk1,2) phosphorylate Lys-Ser-Pro (KSP) repeats in neurofilament proteins NF-H and NF-M. J. Neurosci. 18, 4008–4021.

Vickers, T., Lima, W., Nichols, J., Crooke, S., 2007. Reduced levels of Ago2 expression result in increased siRNA competition in mammalian cells. Nucleic Acids Res. 35, 6598–6610.

Vigne, S., Germi, R., Duraffour, S., Larrat, S., Andrei, G., Snoeck, R., Garin, D., Crance, J., 2008. Specific inhibition of orthopoxvirus replication by a small interfering RNA targeting the D5R gene. Antivir. Ther. 13, 357–368.

Weber, E.S., Waltzek, T.B., Young, D.A., Twitchell, E.L., Gates, A.E., Vagelli, A., Risatti, G.R., Hedrick, R.P., Frasca, S., 2009. Systemic iridovirus infection in the Banggai cardinalfish (*Pterapogon kauderni* Koumans 1933). J. Vet. Diagn. Invest. 21, 306–320.

Whitley, D.S., Yu, K., Sample, R.C., Sinning, A., Henegar, J., Norcross, E., Chinchar, V.G., 2010. Frog virus 3 ORF 53R, a putative myristoylated membrane protein, is essential for virus replication *in vitro*. Virology 405, 448–456.

Xie, J., Lu, L., Deng, M., Weng, S., Zhu, J., Wu, Y., Gan, L., Chan, S.M., He, J., 2005. Inhibition of reporter gene and iridovirus-tiger frog virus in fish cell by RNA interference. Virology 338, 43–52.

Yamauchi, Y., Kiriyama, K., Kimura, H., Nishiyama, Y., 2008. Herpes simplex virus induces extensive modification and dynamic relocalisation of the nuclear mitotic apparatus (NuMA) protein in interphase cells. J. Cell Sci. 121, 2087–2096.

Zhang, Y.J., Wang, K.Y., Stein, D.A., Patel, D., Watkins, R., Moulton, H.M., Iversen, P.L., Matson, D.O., 2007. (2007) Inhibition of replication and transcription activator and latency-associated nuclear antigen of Kaposi's sarcoma-associated herpesvirus by morpholino oligomers. Antivir. Res. 73, 12–23.

Zhang, Y.L., Cheng, T., Cai, Y.J., Yuan, Q., Liu, C., Zhang, T., Xia, D.Z., Li, R.Y., Yang, L.W., Wang, Y.B., Yeo, A.E.T., Shih, J.W.K., Zhang, J., Xia, N.S., 2010. RNA Interference inhibits hepatitis B virus of different genotypes in vitro and in vivo. BMC Microbiol. 10, 214.

Zhiqiang, W., Yaowu, Y., Fan, Y., Jian, Y., Yongfeng, H., Lina, Z., Jianwei, W., Qi, J., 2010. Effective siRNAs inhibit the replication of novel influenza A (H1N1) virus. Antivir. Res. 85, 559–561.

Zhou, Y., Ching, Y.P., Kok, K.H., Kung, H., Jin, D.Y., 2002. Post-transcriptional suppression of gene expression in *Xenopus* embryos by small interfering RNA. Nucleic Acids Res. 30, 1664–1669.